

PROCEEDINGS OF SPIE

[SPIDigitalLibrary.org/conference-proceedings-of-spie](https://spiedigitallibrary.org/conference-proceedings-of-spie)

ACWI: an experiment to image the Cosmic Web from Antarctica

Anna M. Moore, Christopher Martin, Noam C Maitless,
Tony Travouillon

Anna M. Moore, Christopher Martin, Noam C Maitless, Tony Travouillon,
"ACWI: an experiment to image the Cosmic Web from Antarctica," Proc. SPIE
7012, Ground-based and Airborne Telescopes II, 70122A (10 July 2008); doi:
10.1117/12.790281

SPIE.

Event: SPIE Astronomical Telescopes + Instrumentation, 2008, Marseille,
France

ACWI: an experiment to image the Cosmic Web from Antarctica

Anna. M. Moore^{*a}, Christopher Martin^a, Noam C. Maitless^b, Tony Travorouillon^a

^a Caltech Institute of Technology, 1200 E California Blvd, Pasadena, CA, USA 91125

^b Harvard Graduate School of Design, 48 Quincy Street, Cambridge, MA, USA 02138

ABSTRACT

The Antarctic Cosmic Web Imager (ACWI) is a dedicated 2m-class telescope specifically designed to discover and map resonance UV line emission from the Intergalactic Medium (IGM) and to explore the low surface brightness universe. IGM mapping will provide a new measurement of large-scale structure and the distribution of dark matter over a large and unique range in overdensity. The South Pole provides a location with (1) a target elevation that is constant during observation hence sees constant airmass (2) the lowest measured extinction of any ground based site (3) a low and constant ecliptic elevation and hence zodiacal emission away from the target location and (4) long duration nights yielding stable sky and instrument properties enabling the required accurate sky subtraction. These factors combined imply a sky background that is the most stable of any ground-based site, a requirement for this particular science case where the subtraction of sky background, rather than the image quality, must be exquisite. We present the baseline instrument design that is catered to perform this science case only and is not a general purpose instrument, increasing robustness and reliability.

Keywords: Antarctica, Cosmic Web Imager, IFU spectrograph, image slicer

1. ACWI SCIENCE OBJECTIVES

Recent, spectacular measurements of the cosmic microwave background have provided strong constraints on cosmological parameters. The initial conditions that led to structure formation in the Universe are becoming clear: the geometry of the Universe (flat), the origin of flatness, homogeneity and scale-invariant fluctuations (Inflation), the density of baryons $\sim 4\%$. Combined with local dynamical measurements, we now can assess the basic constituents of mass-energy today: 70% dark energy, 26% dark (non-baryonic) matter, 3% "unseen" baryons, $\sim 1\%$ baryons in visible galaxies.

At the same time, while the initial conditions are coming into sharp focus, the physical processes that built structure and galaxies that delineate that structure remain obscure. After becoming non-linear (overdensity $\delta = \Delta\rho/\rho > 1$) regions of local overdensity collapse to form virialized, self-gravitating halos ($\delta \sim 200$). The dark matter halos accrete other dark matter and baryons into their potential wells. While dark matter cannot dissipate this potential energy, baryonic matter can--as it collapses it heats and radiates, becoming more tightly bound and compact. Thus the properties of galaxies must be directly tied to the behavior of gas dissipating and cooling within the dark matter halos. Ultimately this cooling gas becomes dense enough to form stars. Massive stars produce energetic winds and supernova explosions, which inject energy and heavy elements back into the gas, the halo, and the surrounding IGM. These processes are very poorly understood.

Computer simulations are still far from being able to trace structure and galaxy formation on the wide range of physical scales required. Simulations can model large-scale structure growth, or can with initial conditions model the evolution of a proto-galactic region (with fundamental uncertainties). Semi-analytic models combine N-body simulations to predict large-scale structure with heuristic recipes for galaxy formation and evolution: rules for gas shocking, cooling and dissipation, star formation, halo and galaxy merging, and feedback fraught with many free parameters that cannot be determined from first principles. While this approach has led to considerable success in matching the statistical properties of observed galaxies, a deep physical understanding of galaxy formation and evolution remains an elusive goal.

Observational efforts are primarily focused on using large multiwavelength galaxy surveys to measure properties at low and high redshift. While galaxies are the most visible lighthouses tracing the architecture of the Universe, the stars in them represent less than 1% of the mass density of the Universe. The IGM directly traces the 4% of baryons, and

indirectly the 26% of dark matter in the universe. At the same time, the IGM provides major new insights into galaxy formation and evolution.

1.1 A comprehensive study of the IGM

We propose to study an Antarctic-based telescope-instrument concept, the Antarctic Cosmic Web Imager (ACWI), designed to map IGM emission over significant cosmic volumes at the peak of cosmic star formation ($z \sim 2.5$) with unprecedented sensitivity and spatial resolution. Mapping emission from the IGM will provide the first 3D map of large-scale structure directly tracing low and moderate overdensities ($\delta \sim 10$ –300), the first map of the reservoir of gas that fuels galaxy formation and evolution, the first comprehensive measurement of the metagalactic background and its spatial uniformity, and the first large-scale search for the emission signature of galactic and AGN feedback on the IGM. Coupled with a companion redshift survey (obtained at a general purpose Southern observatory), along with QSO absorption line spectra obtained over the same cosmic volume, the IGM map can be cross-correlated with the distribution of galaxies and QSO absorption lines. The map will provide a complementary and unique view of the evolving universe, the physical properties of the IGM, and the interrelationship of galaxies, AGN and the IGM.

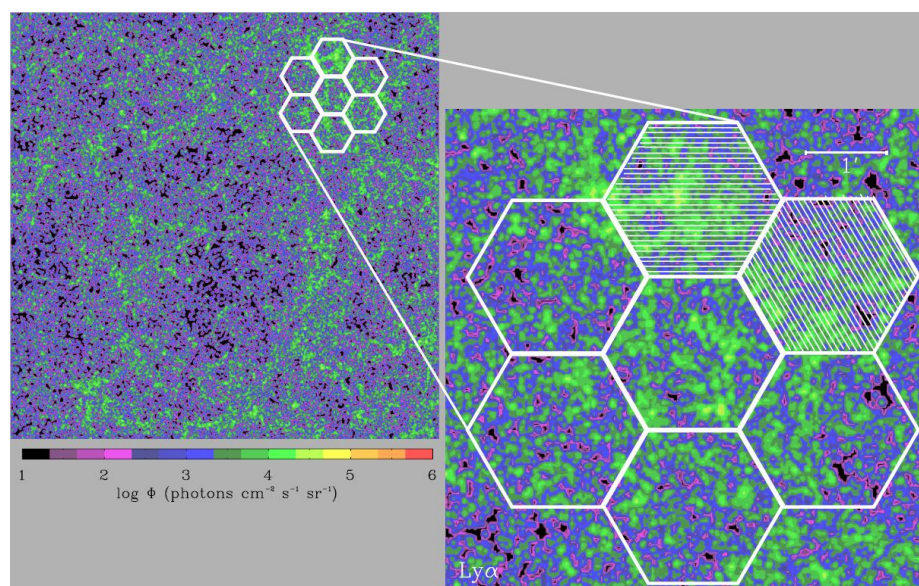


Figure 1. Predicted Lyman α emission line distribution for a simulation provided by S. Furlanetto [1]. The volume is centered at redshift $z \sim 2.5$ and has thickness of $\Delta z \sim 0.07$, (~ 10 nm, 1/3 of the ACWI band-pass) The left panel shows a 17×17 arcmin² area ($1/16^{\text{th}}$ of the total area of the WLS), the right panel shows an enlargement of the selected box comparable to the deep survey (DLS) area. The six IFU/spectrograph fields are shown, two with slits. The dark and multiphase baryonic matter simulation was done with the smoothed particle hydrodynamics (SPH) GADGET code [2] using the fully conservative entropy formulation [3]. The model accounts for variations in density, temperature, photoionization, self-shielding and metallicity, including galaxy feedback effects. Blue and green regions are detectable in the WLS, and purple in the DLS.

Mapping the Cosmic Web over cosmologically significant volumes and depths requires a dedicated instrument and telescope approach. An Antarctic site is optimal for UV observations (where IGM emission is brightest) and observations limited by sky subtraction systematics. The telescope and instrument can be designed simply but optimally to obtain this unique, breakthrough cosmic map by exploiting the excellent site properties. Our design is focused and robust. A 5 year survey will yield the following results:

Wide Ly α Survey (WLS): A 1 deg^2 map of IGM emission tracing HI in virialized halos with $\delta \sim 100$ –1000 (sensitivity 1000 LU^1) spanning a comoving cosmic volume of 10^6 Mpc^3 at $z \sim 2.0$. We should detect $\sim 10^4$ – 10^5 Ly α emission regions. [2 years]

¹ $1 \text{ LU} = 1 \text{ ph cm}^{-2} \text{ s}^{-1} \text{ sr}^{-1} = 12 \mu\text{R} = 2 \times 10^{-22} \text{ erg cm}^{-2} \text{ s}^{-1} \text{ arcsec}^{-2}$

Deep Ly α Survey (DLS): A 6 x 6 arcmin² deep survey that will map the cosmic web of IGM filaments ($\delta \sim 10$ -100, sensitivity 100LU) in emission over a cosmic volume of 10⁴ Mpc³, detecting $\sim 10^3$ -10⁴ emission regions. [2 years]

Ly α Evolution Survey (LES): A 10 x 10 arcmin² map of Lyman α emission regions at $z \sim 3.0$, in order to study the evolution of the IGM (sensitivity 1000LU). [1 year]

OVI/Ly α Survey (OLS): Wide-field and deep maps of OVI1033 emission tracing warm ionized gas in halos and cosmic web filaments, and radiative shocks from galactic winds striking the ambient IGM, at $z=2.5$. [1, 3]. This will couple with a smaller area survey of Lyman α at $z=2.5$ to correlate the relative distribution of Ly α and OVI.

Our estimates above are based on direct detection of 10 arcsec diameter emission regions in the blank field survey. The predicted intensities are based on simulations of Furlanetto et al. [2], Cantalupo et al. [5], and our own estimates. While the physics of the OVI emission models is complex and uncertain, the Ly α emission estimates are quite simple and reasonably secure. A simulation example is shown in Figure 1.

Our survey region will be chosen to have comprehensive galaxy redshift surveys over $2 < z < 3$. The WLS and DLS will each contain ~ 10 QSOs that will provide absorption line spectra in the primary survey data set. With these it will be possible to:

1. Stack on galaxy centers to reach a factor of 10-100 lower emission strengths.
2. Stack on predicted filaments connecting galaxies to reach 10-100 lower emission strengths.
3. Cross-correlate IGM emission with galaxies (measure IGM-galaxy cross-correlation ξ_{GI}).
4. Cross-correlate IGM emission and absorption in the QSO spectrum (equivalent to stacking in redshift space).

With the exquisitely low systematic errors enabled by the dedicated instrument and Antarctic site, these techniques may allow us to probe overdensities as low as $3 < \delta < 30$. Our survey potentially spans more than three orders of magnitude on scales as small as 70 kpc (10 arcseconds at $z=2$).

2. ACWI INSTRUMENT DESIGN

We are developing an Antarctic Cosmic Web Imager (ACWI) to detect and map emission from the IGM from the South Pole. Observations at a range of redshifts will be necessary to form a complete evolutionary picture of the IGM. ACWI will observe the strong, redshifted UV resonance lines of Ly α 121.6, CIV 155, and OVI 103 at moderate redshift. We are targeting observations in the U and B bands (the “blue”, 350nm-500nm baseline) therefore the low and stable background conditions found on the Antarctic plateau offer the greatest performance in terms of sky background subtraction. IGM emission will be extended and much fainter than the foreground diffuse emission. It will only be detected by dedicated instruments optimized for low surface brightness, wide field emission line surveys in the presence of time and spatially variable diffuse foregrounds. This driving requirement has led to our proposed South Pole site and the baseline instrument design we discuss below. A summary of the science requirements is shown in Table 1.

2.1 Why observe in the “blue”?

IGM emission is brightest at UV wavelengths, because of surface brightness dimming and the drop in the QSO and ionizing flux density at $z > 2.5$ (Ly α falls by a factor of 3 from $z=2$ to $z=3$ and another factor of 5 from $z=3$ to $z=4$). Atmospheric transmission at a ground based location limits the minimum wavelength to ~ 320 nm.

Exquisite sky subtraction is required to directly image the faint IGM emission, as well as exceptionally good instrument systematics. Sky background is in general composed of (1) continuum emission consisting of zodiacal light, integrated starlight, scattered sunlight from the moon and sun in non-dark time conditions, scattering from cirrus and diffuse galactic light and (2) discrete spectrum emission from atomic and molecular species in the high mesospheric layer, commonly termed airglow that at polar sites includes auroral emission.

Many factors combine to give the resulting sky emission for a particular area of sky over a particular wavelength region of interest. For visible wavelengths, these factors include extinction, aerosol content, altitude of the observation, position angles of the ecliptic, sun and moon, variation in airglow and solar cycle. At a temperate observatory where one tracks over a range of elevation angles the sky background varies both spatially and temporarily. For the U and B photometric

bands, however, the sky background magnitude is the lowest. The sky is darkest in the U band and varies little between temperate sites (22.5mag/arcsec^2 Paranal during dark time [6], 22.6mag/arcsec^2 for Mauna Kea during dark time [7]).

The broadband sky background temporal variability is lowest in the U band (0.1mag/arcsec^2 [7], 0.3mag/arcsec^2 [6]). This is likely due to the reduced airglow emission experienced at these wavelengths compared to wavelengths redder than $\sim 500\text{nm}$ (O_2 Hertzberg band spectrum rather than OH Meinel band emission). For the U and B bands the relative contribution of airglow emission and continuum are comparable, while redward of 500nm the more spatially and temporarily varying airglow emission dominates. This is evident in the diffuse sky background measurements above the Calar Alto site shown in Figure 2.

2.2 Aurora

The South Pole is located underneath the auroral oval and as such experiences substantial auroral activity. The strongest lines lie redward of 700nm [44], however, weaker emission due to the second positive bands of N_2^+ ($350\text{--}400\text{nm}$) and first negative bands of N_2^+ ($400\text{--}500\text{nm}$) exist. These lines are distinct to airglow though for the purposes of this experiment provide the same problem: a spatially and temporarily changing background. The solution is an instrument with sufficient spectral resolution to resolve between the auroral lines combined with targeting bands absent of any auroral (or airglow) emission. ACWI is designed specifically for this purpose.

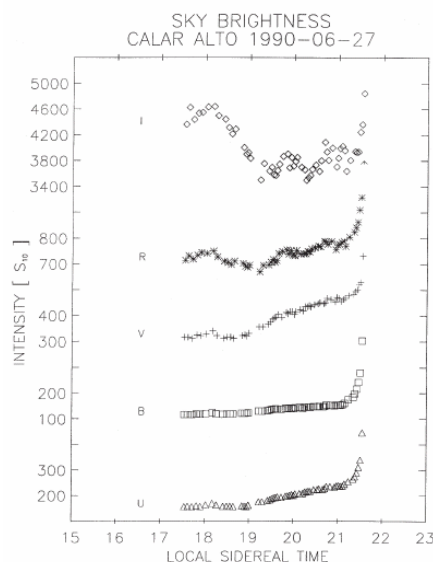


Figure 2. The diffuse sky background measured above the Calar Alto site in each of the UBVRI bands as a function of time. The stability of the U and B bands is very evident. [30].

2.3 Why a South pole location?

In order to image the cosmic web, a 1 sigma subtraction error $< 2 \times 10^{-4}$ must be achieved (in order to make the systematic error < 0.5 the Poisson error for a signal of 100LU predicted for $\text{Ly}\alpha$ in the web vs. 50,000 LU in the continuum). ACWI is not an experiment that requires exceptional seeing, rather exceptional stability of both background and instrument. Crucial to the successful removal of sky background to this level are (1) a low and stable continuum background (2) continuous observing nights (3) constant elevation of the target (4) low and uniform temperatures and (5) almost perfect instrument systematics such as zero flexure. A South Pole location fulfills these requirements more than any other ground based site as (1) The aerosol content above the South Pole is the lowest measured at any ground based site (optical depth: 0.03 [29]). Aerosols are a major contributor to broadband scattering processes in the troposphere that increase and vary the background level, a significant contribution in the U and B bands; (2) The South Pole is the only ground based location where one can observe at a fixed elevation and hence a fixed air mass and extinction; (3) The ecliptic is always low and constant from the South Pole. Scattered light from zodiacal dust is a major contributor to continuum sky background at U and B wavelengths; (4) The South Pole offers a site with extended periods of astronomical twilight conditions during the winter season with a low lunar maximum altitude ($< 30^\circ$). Altitude over azimuth and equatorial arrangements are equivalent at the South Pole. ACWI does not require a field de-rotator, can

adopt a single, constant speed motor for tracking, can keep all optical components stationary with respect to one another during tracking and most importantly keep all optical components fixed with respect to gravity.

2.4 ACWI Optical Design

A schematic of the baseline concept for the ACWI is shown in Figure 3. The optical design consists of (1) a plano-mirror (TM1) of maximum dimension 2.8m (minimum 2m) that directs light from a zenith range of 0° to 45° (baseline) along the horizontal optical axis of the instrument (2) a Cassegrain system (TM2 primary, TM3 tertiary) that produces a F/20 feed and 5 arcmin field of excellent image quality (3) a dichroic splits the optical feed, reflecting the blue to a vertically orientated IFU spectrograph while feeding an acquisition and guide camera in direct feed mode. The optical performance of the telescope feed is excellent across the field, as expected from a Cassegrain design. With a slight curvature of the field ($\sim 0.3\text{m}$ radius of curvature) the imaging performance is sub-diffraction level for a 2m class telescope, though is not required for this science case.

2.5 ACWI Opto-mechanical design

The mechanical layout consists of a horizontal rotating platform onto which all the optics are located as shown in Figures 3-6. Only 2 components move with respect to the platform for acquisition and during an observation: (1) TM1 rotates in elevation to acquire a target but is fixed during observation (2) the spectrograph rotates in between observations by 60° to perform the novel “rotate and shift” procedure for sky background subtraction (see below) and (3) the guide camera and the TM3 active tip-tilt stage (therefore slow moving) work harmoniously to keep the target centered on the spectrograph field center. TM3 is close enough to the pupil that rotation of this element produces negligible movement of the pupil image at downstream optics such as the grating. The rotating platform rotates continuously and at a constant speed during tracking, only requiring to de-rotate once per day (to prevent cable entanglement).

For this application the large TM1 mirror can be segmented, for example into 4 mirrors of cross-section roughly 1.4m by 0.5m. This may increase the mirror cell complexity of course and therefore a careful trade study is required.

This arrangement, though requiring an extra large flat siderostat to feed the 2m Ritchey-Chretien system, enables the ACWI instrument to have all components be *fixed relative to gravity during an observation*. This is particularly important for the multi-component spectrograph and large mirrors.

2.6 ACWI Enclosure design

The enclosure is based on a standard commercial shipping container with outside dimensions of 45ft (length) by 8ft (width) by 9ft6 (height). The container is modified to provide doors at either end for access as shown in Figures 4. The roof and baffling design is of considerable importance and is shown in concept form only in Figure 4. The entire shipping container, modified roof and internal components are mounted on a rotation bearing that provides the azimuthal rotation required for tracking an object as shown in Figure 6. Any error in the pointing, that is required to be sub-arcsecond level, is corrected using the servo-combination of the guide camera and TM3 tip-tilt stage.

2.7 ACWI Spectrograph Design

For the ACWI experiment, a VPH (Volume Phase Holographic) grating spectrograph with IFU is superior to other approaches, in particular a fabry-perot spectrograph or a scanned long-slit spectrograph. Fabry-perots require scanning in time over wavelength, mixing temporal and wavelength-dependent systematics, reducing the integration time over the entire wavelength band, and requiring complex precision etalon controllers. In our application, a broader band spectrum is desirable since metal line complexes may have multiple components spread over 500 km/s and faint lines will be confirmed only by detection of doublets. A moderate band of the spectrum provides important information about the various background sources and whether they are being effectively subtracted. A fabry-perot with a finesse of 30 would provide a free spectral range of only 3\AA . Long-slits require temporal scanning to map the Cosmic Web. With the VPH design we can obtain a very deep exposure (DLS) over the bandpass without scanning, and also perform a survey type observation (WLS).

The ACWI baseline spectrograph design consists of a long-slit VPH spectrograph operating in a single order at a $\sim 45^\circ$ incidence angle. The long-slit is fed by an Integral Field Unit (IFU) to provide $300 \times 300 \text{ arcsec}^2$ field of view. The field of view is divided into an array of 6 hexagonal fields each covered by a ~ 30 reflective slit IFU (Figure 1) and a dedicated long-slit spectrometer channel consisting of a simple reflective collimator, VPH grating, and UV-optimized refractive camera. The f/2 camera will be a simplified (for narrowband operation) and significantly reduced adaptation of

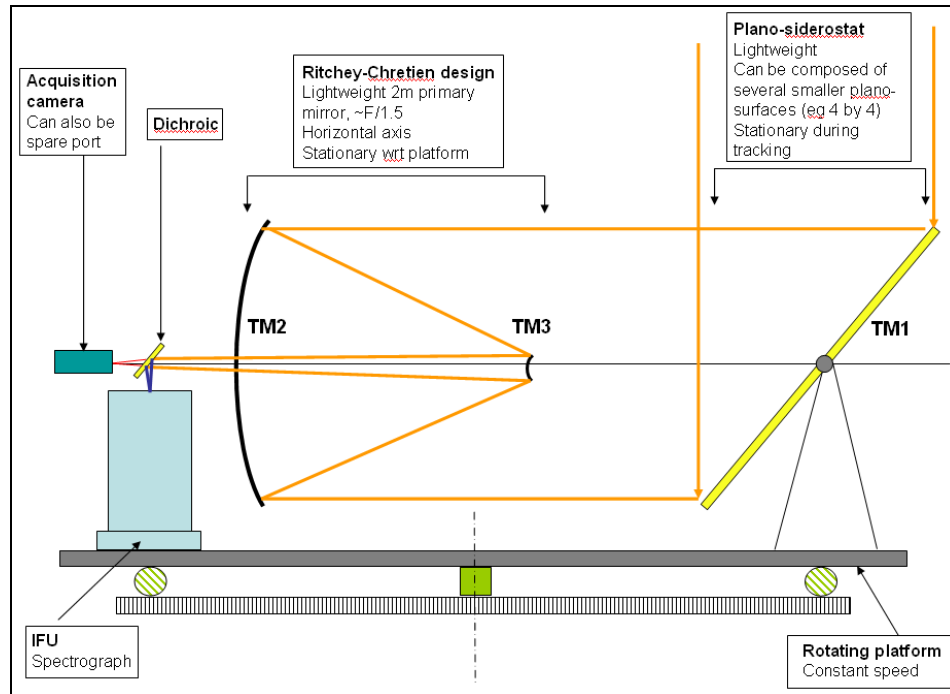


Figure 3. A schematic of the baseline design for the Antarctic Cosmic Web Imager. ACWI contains no elements, optical or otherwise, that move in a changing gravity field during an observation, so producing a system with zero flexure variation.

Table 1. Science Requirement Flowdown

	Baseline	Minimum	Optimum
Bandpass	3500-5000Å	3500-3800Å	3300-6000Å
Instantaneous bandpass	300Å	250Å	350Å
Field of view	5 x 5 arcmin	3 x 3 arcmin	8 x 8 arcmin
Zenith angle	0 to 30°	0 to 30°	0 to 45°
Azimuth rotation	360°	360°	360°
Spatial sampling [diffuse]	3.1 x 3.1 arcsec ²	3 arcsec	1-3 arcsec
Spatial sampling [point]	3.1 [slit] x 0.8 arcsec ² [CCD]	1.0 arcsec	0.5 arcsec
Background subtraction	Shift [CCD] & Rotate [Field]		
Frame time	30 minutes		15-60 minutes
Cosmic ray fill factor	<3%	<5%	<1%
Rotation "chop" frequency	2 per minute	1 per few minutes	1 per minute or even less
Spectral resolution	5000	4000	6000
System Efficiency	0.2	0.15	0.25
Observational Efficiency	0.7	0.5	0.8
Dark time on single target/year	900 hours	700 hours	1200 hours
Error sys. effects, single target	<2e-4	<5e-4	<1e-4
Survey Length	6 years	2 years	10 years

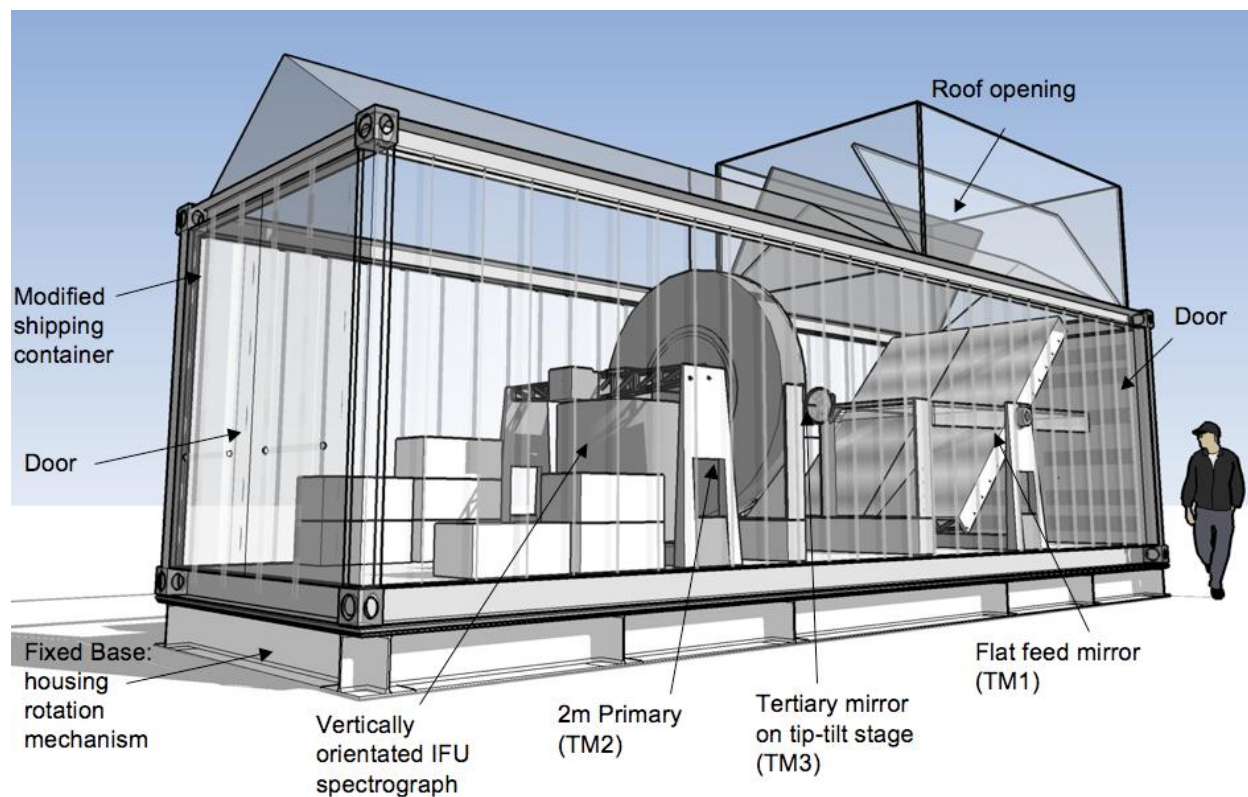


Figure 4. Concept for the ACWI enclosure that is based on a standard sized shipping container with internal opto-mechanical components highlighted. The roof is modified to incorporate a remotely controlled opening above the plano-mirror. The container is mounted to a rotation bearing that provides the necessary azimuthal rotation.

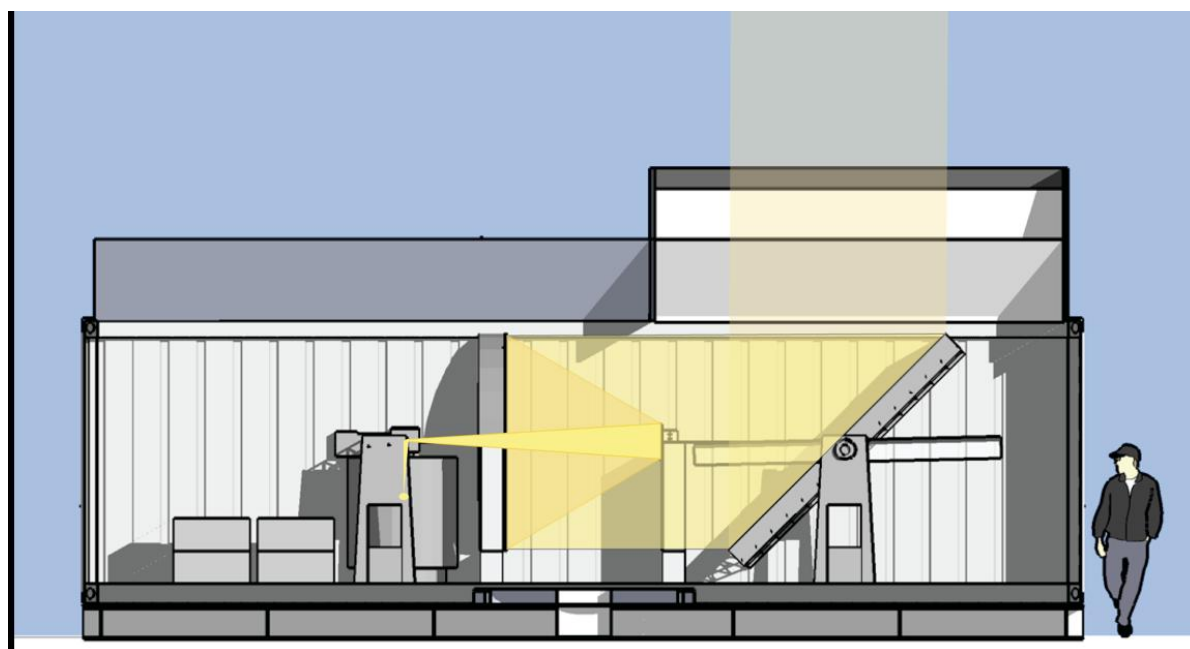


Figure 5. A side view of the main components of ACWI with the optical path highlighted. The plano-mirror is orientated at an elevation of 45 degrees to enable zenith pointing.

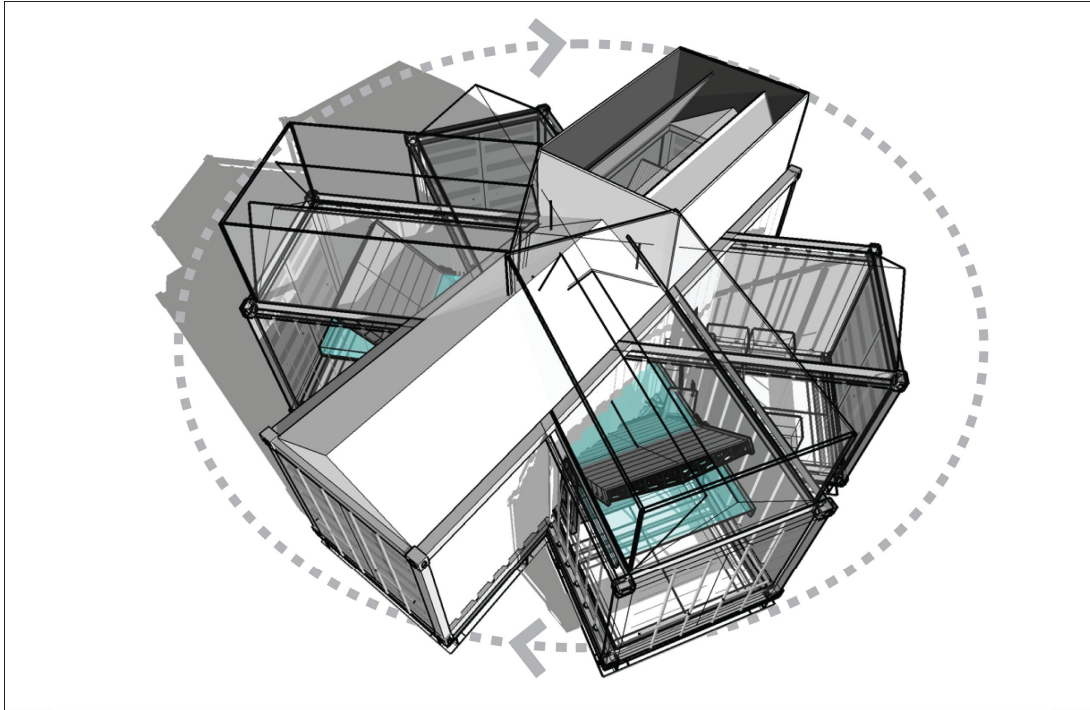


Figure 6. The rotation bearing located underneath the shipping container provides the slow azimuthal rotation for target tracking. The instrument is shown positioned at 3 superimposed rotation angles above.

the Keck/LRIS-Blue camera. Source/background shift-and-rotate and careful attention to systematics provides Poisson-limited sky subtraction.

High resolution is required to provide the best possible source/background subtraction of complex nightglow, aurora and zodiacal light spectra, sufficient contrast between faint IGM lines and the continuum sky background, to resolve IGM lines from complex continuum and airglow band features, and to kinematically separate IGM/PGM components. A ~ 60 km/s resolution ($R \sim 5000$, to be studied) is good for detecting a range of IGM lines, subtracting foreground zodiacal and airglow emission, and separating metal line complexes, based on our simulations and the absorption line profiles obtained by Keck/HIRES.

2.8 ACWI Detectors

The baseline CCD Detector is a Mike Lesser 60 mm x 60 mm state of the art UV enhanced 4,096 x 4,096 pixel CCD with 15 micron pitch and 2.5 electron read noise. The device has a QE of 75% at 350 nm. The low read noise is critical for making the high resolution spectra sky noise limited in a reasonable amount of time. In survey mode (WLS) this occurs in about 30 minutes using 2 by 4 pixel binning. We will adopt a variation of the CCD/telescope shift/nod strategy first used by Sembach [11] for extended sources (and related to the nod-and-shuffle technique for point sources of [13]). In this scheme the CCD divided into exposure regions (middle 1/3 in one dimension) and storage regions (outer 2/3). Source and sky spectra are obtained alternatively, and while the spectrum is being shifted into its storage area the telescope is repointed to either the source or sky location. This permits a rapid sampling of source and sky (reducing the impact of temporal variations) while reaching sky-limited exposures, and ensures that source and sky spectra are obtained through an identical instrument path.

This approach works well if the time for clocking through the CCD is much shorter than any airglow variation timescales. We have employed cyclic clocking for our Pulsar camera (e.g., [15], [16]), with periods as short as 30 msec. For this application cycle times depend on the airglow temporal power spectrum. We use measurement of OH Meinel bands as guidance, since O_2 bands exhibit behavior similar to OH [12]. Based on the power spectrum amplitude and slope of [14], and assuming that O_2 bands dominate the background, we require roughly one cycle per minute, to reduce the residual subtraction error to the design value shown in Table 1. There is the option of tracking with a guide camera located in the central channel of the spectrograph if this has merits over the baseline design.

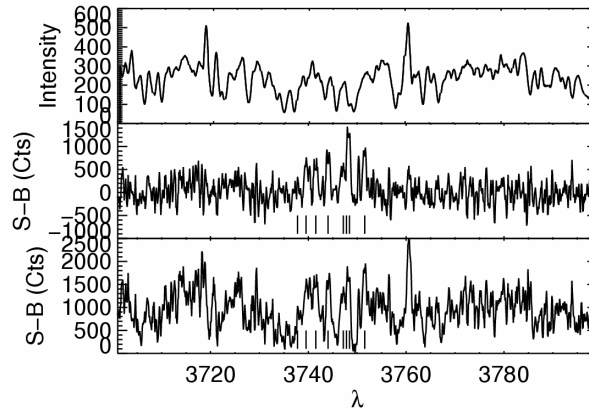


Figure 7. TOP: Simulated source (airglow [NO, O₂] plus zodiacal and diffuse galactic light and IGM lines) spectrum observed at R=5000 in LU * 1/100, including emission from eight Lyman alpha regions spanning ~1000 km/s indicated by vertical lines, at redshift z=1.84, with intensities I=60-300 LU, occupying an area of 100 arcsec². MIDDLE: Simulated source-background spectrum in Deep Survey (DLS). All lines >100LU are easily detected. BOTTOM: Same as middle panel with 1% error in sky subtraction. All lines are now indistinguishable from noise.

3. BACKGROUND SUBTRACTION & CONTROL OF SYSTEMATICS

Given that sky background (more accurately foreground) is 100-1000 times brighter than IGM emission, and because IGM emission is extended and nominally in unknown locations, we have developed a novel approach to sky subtraction in which the site, telescope, IFU, spectrograph, detector/electronics, and observing strategy play key roles in an integrated strategy. There are six causes of incorrect subtraction: sky variations in space, wavelength and time, and instrument variations in space, wavelength, and time.

Airglow background in particular varies over the sky, in wavelength, and in time during the observing night. The airglow in the 350-450nm band that we baseline for initial observations is dominated by O₂ (Herzberg and Chamberlain bands) and weak OH {[17], [18], [19]}. These all exhibit spatio-temporal variations due to gravity waves and turbulence propagating through the layer in which the photochemical reactions produce the observed bands {[20], [21], [22], [23]}. The observational strategy must be optimized to either measure or average over these variations. That the source and background are both extended over large, common angular regions is a further annoyance. The rotate and shift strategy is critical for precision sky background subtraction. The impact of inaccurate sky subtraction is shown in Figure 7.

First we discuss how we perform and maximize the accuracy of background subtraction in the presence of these effects (rotate and shift). Then we discuss how we minimize these effects (minimize systematics).

3.1 Background Subtraction

In the 3D survey volume, IGM emission features will occupy a relatively low filling factor, less than 10% for even the faintest cosmic filaments. Thus in any pair of fields, with a reasonable separation that exceeds the typical transverse dimensions of filaments ($\ll 350$ kpc ~ 50 arcsec), a sky-voxel in field 1 observed by a given instrument-voxel can be subtracted from a sky-voxel in field 2 observed by the identical instrument-voxel. (Note that a single instrument-voxel would consist of a single spectral bin and a 10×10 arcsec² spatial region obtained over several IFU slits.) In practice a large number of voxels will be combined to provide the reference ("background") spectrum.

The field of view is divided into six hexagonal subfields arranged in a symmetrical hexagonal array, as shown in Figure 1 and 8. Located behind each hexagonal field is a single small IFU spectrograph consisting of ~30 image slicers. The slicers are oriented tangentially to the rotation axis (Figure 1). Using slight and symmetrical tilts, the six otherwise standard design IFUs (2 reflections) can be colocated with contiguous fields without additional optics. Each spectrograph CCD is divided into exposure regions and storage regions, as discussed earlier. The IFU/spectrograph array can be rotated about the field center (mechanical rotation about the vertical).

During a single integration (typically 30 minutes) we will execute the following (repeated) sequence: 1) expose (position A=spectrograph azimuth 0) for ~1 minute, 2) close shutter, 3) transfer azimuth 0 spectrum to upper storage, 4) rotate IFU-spectrograph 60, 120, or 180 degrees, 5) expose (position B), 6) close shutter, 7) transfer B spectrum to lower

storage, 8) rotate back to position A, and repeat. Note that rotation into mechanically locked azimuth positions will aim to occur in <2 seconds (simultaneous with transfer). A schematic example is shown in Figure 8.

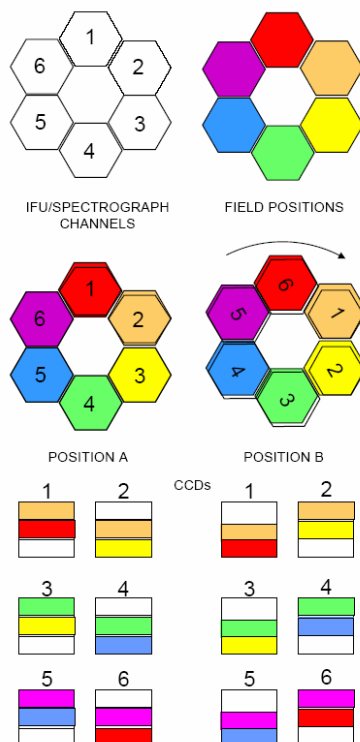


Figure 8. Schematic illustrating rotate and shift method. Numbers correspond to instrument channels, colors to sky subfields. Middle two figures show two positions separated by 60 degrees. Bottom shows 6 CCDs each with storage (upper and lower 1/3) and detection areas (central 1/3).

After 30 minutes, we will have 6 interlocked pairs of spectra corresponding to 6 subfields each observed in two channels. By varying the rotation step (60, 120, or 180 degrees) and phase, a total of 108 pairs (all possible) are accumulated over ~9-12 moonless hours. Every subfield will be observed by all six channels, as part of all possible pair combinations each obtained with ~1 minute temporal separation.

The rotate and shift implementation of sky background subtraction places no extra complexity on the telescope tracking system as compared to a nod and shift procedure where the entire telescope, or part of it, must be repointed. Tracking is maintained by the non-rotating guide camera.

3.2 Control of Instrument Systematics

The control of instrument systematics is unique in the ACWI experiment. Under normal circumstances instrumental non-uniformities, such as varying flexure, pupil shifts, and temperature during the observation, produce errors in the subtraction procedure. For ACWI *sited at the South Pole* no component, optical or otherwise, moves with respect to the gravity vector during an observation. The pupil is symmetric and fixed in each channel at each rotation point. The low and relatively constant temperature during winter at the South Pole and the lack of frequent diurnal variations is another huge advantage to controlling temperature related systematics. Slow long-term variations are well-sampled by shift-and-rotate.

Our observing strategy minimizes foreground and its variation, minimizes scattering of out of field objects, and maximizes the fidelity of sky background subtraction. By performing a large cosmic volume survey, we are ensured of detecting thousands of bright IGM regions in any direction. We will select our survey region to have optimal foreground properties: (1) Low and smoothly distributed cirrus and reflected diffuse galactic light. These will be based on sensitive GALEX observations. Small DGL variations will be calibrated and removed using the backscattered stellar spectrum which should be extremely constant over 1 degree of sky. (2) Low and smoothly distributed UV (Milky Way) extinction.

Small variations can easily be determined and corrected for. (3) High ecliptic latitude. The zodiacal light dominates the sky foreground. Spatial variations are not expected, but the spectrum is complex. Our high resolution spectral sky flat will allow us to remove zodiacal light with high accuracy. (4) No bright stars or nearby galaxies in or near the field, to eliminate scattering wings. Faint stars and galaxies will be masked from the final spectra, and PSF wings are predicted to be a very small contribution.

The field will have a comprehensive redshift/spectroscopic survey at $2 < z < 3$ along with photometric data so that galaxies and AGNs can be identified in the survey volume. Each subfield of the 6 field mosaic will be observed by each spectrograph/IFU channel. The WLS will provide 13,000 subfields each observed by all 6 channels. This will permit the generation of a super spectral sky flat.

Direct detection of emission regions is possible in the WLS to 1000LU and in the DLS to 100LU. As discussed earlier, in order to reach even deepest sensitivities we will stack on galaxy centers and predicted filaments from the redshift survey to reach a factor of 10-100 lower emission strengths and cross-correlate IGM emission with galaxies and QSO spectra (stacking in redshift space).

4. SUMMARY

We present a concept design for a 2m-class telescope optimized for direct detection and mapping of UV resonant line emission from the Intergalactic medium (IGM) and to explore the low surface brightness Universe. The success of the experiment is based on obtaining exquisite sky background subtraction in the optical U and B bands. We choose to locate the experiment at the unique South Pole location so that we can eradicate instrument-induced variables that exist at any other non-polar ground based location and benefit from the potentially low sky background variation.

REFERENCES

- [1] Furlanetto, S.R., Schaye, J., Springel, V., & Hernquist, L. 2005, *Astrophysical Journal*, 622, 7
- [2] Furlanetto, S.R., Schaye, J., Springel, V., & Hernquist, L. 2003, *Astrophysical Journal Letters*, 599, L1
- [3] Springel, V., & Hernquist, L. 2002, *Monthly Notices of the Royal Astronomical Society*, 333, 649
- [4] Furlanetto, S., Schaye, J., Springel, V., & Hernquist, L. 2004, *Astrophysical Journal*, 606, 221
- [5] Cantalupo, S., Porciani, C., Lilly, S.J., & Miniati, F. 2005, *Astrophysical Journal*, 628, 61
- [6] Patat, F., private communication, 2006
- [7] Steidel, C., private communication, 2006
- [8] Meinel, A.B, 1951 *Rep. Prog. Phys.* 14 121-146
- [9] Jefferson, A., NOAA, private communication, 2006
- [10] Leinert, Ch., et al., The 1997 reference of diffuse night sky brightness, *Astron.Astrophys. Suppl.Ser.* 1998, 127,p1-99
- [11] Sembach, K. R., Tonry, J. L., Accurate sky Subtraction of Long-Slit Spectra: Velocity Dispersions at $\Sigma(v) = 24.0 \text{ Mag/arcsec}^2$, *Astronomical Journal*, 1996, v.112, p.797
- [12] Barbier, D. 1956, *Special Suppl. No 5 to the J. Atm. Terr. Phys.*, p38
- [13] Glazebrook, K., Bland-Hawthorn, J., 2001, *PASP.* 113. p 197
- [14] Hecht, J.H., et al., *Geo. Res. Lett.*, 1995, 22, p 2873
- [15] Kern, B., Martin, C., Optical pulsations from the anomalous X-ray pulsar 4U0142+61, *Nature*, 2002, 417, p 527
- [16] Kern, B., Martin, C., Optical Pulse-Phased Photopolarimetry of PSR B0656+14, *ApJ*, 2003
- [17] Krassovsky, V.I., Shefov, N.N., & Yarin, V.I., 1962, *Planet. Space Sci.*, 9, 883.
- [18] Broadfoot, A.L., Kendall, K.R., 1968, *JGR*, 73, 426
- [19] Osterbrock, D.E., Waters, R.T., Barlow, T.A., Slanger, T.G., & Cosby, P.C., 2000, *PASP*, 112, 733
- [20] Hines, C.O. 1960, *Can. J. Phys*, 38, 1441
- [21] Yamada, Y., Fukunishi, H., Nakamura, T., & Tsuda, T. 2001, *Geo. Res. Lett.*, 28, 2153
- [22] Ejiri, E., et al. 2001, *JGR*, 106, 22793
- [23] Stockwell, R.G. & Lowe, R.P. 2001, *JGR*, 106, 17185